A Curved Mortise-Tenon Timber Joint for Robotic Non-sequential Assembly with Reinforcement Learning

Lingyue Wu[1] and Anja P. R. Lauer[1]

[1]Institute of Construction Materials, University of Stuttgart, Germany
lingyue.wu@iwb.uni-stuttgart.de, anja.lauer@iwb.uni-stuttgart.de

Abstract –

Robotic assembly of timber structures promises increased efficiency and sustainability in construction. However, conventional timber joints often cause high assembly difficulty for robots (e.g. bolts) and use non-reversible connectors (e.g. nails or glue). This paper presents a novel curved mortise-tenon timber joint designed for robotic non-sequential assembly and a dual-arm assembly strategy based on reinforcement learning (RL). The joint's curved and non-sequential geometry enables full reusability, kinematic self-locking, and improved stress distribution under loading. To robustly execute the complex insertion in the presence of uncertainties, an RL policy trained via Proximal Policy Optimization (PPO) with extensive domain randomization is employed. In physical experiments with two Franka robot arms, the learned policy achieved a 90% success rate in assembling and disassembling the joint, validating the approach. The results demonstrate that combining innovative joint design with learning-based control can advance automated circular construction by enabling robotic assembly and disassembly of timber joints.

Keywords –

Timber joint; Automated assembly; Automatic construction; Mortise-tenon; Reinforcement learning; Reusability

1 Introduction

The construction industry faces the challenges of improving sustainability and addressing labor shortages [1]. Timber construction is resurging as a sustainable alternative to steel and concrete, since wood is a renewable material with a lower environmental footprint [2]. Timber engineering leverages digital fabrication to create precise components, enabling innovative structural systems with reduced carbon emissions [3]. An aging population has led to labor shortfalls in construction. Robotic on-site assembly can help fill workforce gaps and boost productivity [4][5][6]. Robots can handle repetitive tasks with high precision and operate in hazardous environments, improving safety and efficiency in construction.

In pursuit of sustainability, reversible timber joints are developed [7] to allow structural members to be disassembled and reused at end-of-life instead of being demolished, enabling circular construction. For example, [8] introduced a reversible timber beam connection designed for robotic assembly and disassembly. Their connection uses steel bolts as demountable fasteners, providing reliable load transfer while allowing the timber to be taken apart and reassembled multiple times without damage. However, the robotic system in [8] needed to insert and tighten screws with high accuracy. On a construction site, achieving the fine alignment needed for bolts can be difficult due to tolerances, material swelling, or measurement errors. Even millimeter-scale deviations can hinder bolt insertion, demanding a level of accuracy that is hard to guarantee. Thus, although bolted reversible joints work, the installation process is not ideal for robots operating in imperfect site conditions, as it may require slow, careful alignment or human intervention.

To improve feasibility of robotic assembly, researchers have explored non-sequential timber joints as an alternative. A non-sequential joint is a form-fit connection that can be assembled without additional fasteners or glue, relying purely on geometric interlocking of the timber elements (often via mortise and tenon-like features) [9][10]. Unlike traditional sequential assemblies, where components are added one after another in a fixed order, non-sequential assemblies involve moving all parts simultaneously into place, locking them through kinematic constraints rather than friction or hardware. Glath et al. [9] demonstrated that such joints can be designed to self-lock by their geometry, allowing low-force, damage-free assembly and disassembly, since no nails or adhesives bind the parts. Additionally, by eliminating glue and screws, the assembly process is simplified for robots, as there is no need for drilling, nailing, or curing time.

Despite their advantages, existing non-sequential joints have limitations due to the straight tenons. The multi-tenon arrangement constrains the allowable tenon length and cross-section, as several connectors must be accommodated without mutual interference. Thus, the effective load-bearing overlap between members is limited, which can compromise structural performance. Under bending, the contact area is often small and stresses concentrate around the short tenons, reducing the joint's moment capacity. Also, repeated vibration can promote gradual separation as small clearances accumulate over time.

To overcome these problems, this work proposes a novel curved mortise-tenon joint geometry for non-sequential joints. The curved tenon provides greater embedment length for improved mechanical engagement, and it distributes stresses more evenly along the curve when the joint is bent.

However, introducing a curved, non-sequential mortise-tenon joint creates new challenges for robotic assembly. Unlike straight insertions, assembling a curved interlocking joint requires all mating parts to move simultaneously along a precise curved path, which is a complex contact-rich manipulation problem. Moreover, real construction environments have inherent tolerances: timber pieces may be positioned a few millimeters off, and exact trajectories are hard to repeat on site.

Reinforcement learning (RL) can achieve high success rates in complex peg-in-hole insertions [11][12]. This research leverages RL as a control strategy to robustly handle the requirements for coordinated motion, complex contacts, and uncertainties. RL enables the robots to learn an assembly policy through simulation and adapt to contact feedback, rather than relying solely on closed-loop position commands. By training in a varied environment, an RL policy can also become tolerant to small positioning errors or part variations, making it well-suited for the unpredictability of robotic assembly. Compared to assembly methods that rely solely on fiducial markers (as in [13], which reported mixed success for multi-tenon assembly), this research uses AprilTag only for coarse initial localization. The fine alignment and contact adjustments are then handled by the RL-based policy.

The contributions of this work include the introduction of a novel curved non-sequential mortise-tenon timber joint (Figure 1 a, b), that is structurally robust and fully reversible, requiring no metal fasteners or adhesives and thereby supporting circularity and reuse. Further, an RL-based dual-robot control approach for the assembly and disassembly of the proposed joint is presented, which learns coordinated insertion motions through training in simulations to handle complex contact interactions and uncertainties. The results of real robot tests demonstrate that the combined joint-method framework enables robust, tolerance-aware robotic assembly and disassembly of timber joints, advancing automation-friendly and sustainable timber construction. A video showing the real tests is available at [14].

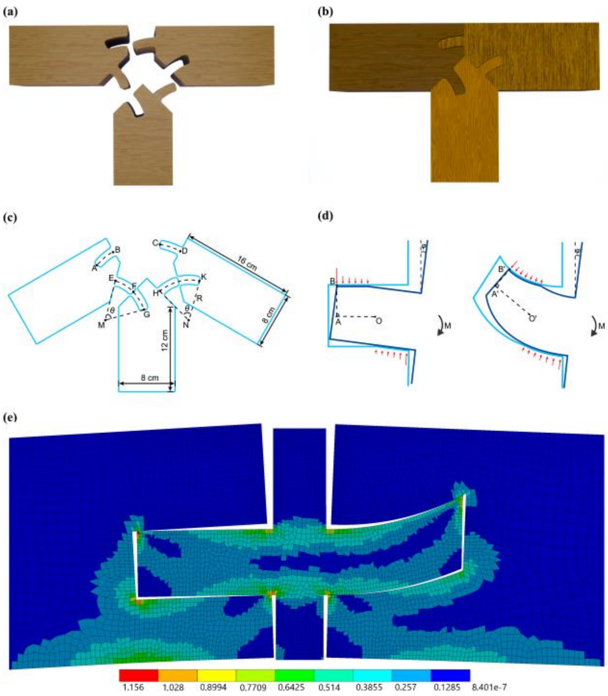

Figure 1. Design of the curved mortise-tenon joint. (a)-(c) Joint design and geometry. (d) Geometric comparison of straight and curved tenons. (e) Von Mises stress distribution (in MPa) of a finite element analysis for comparison of straight and curved mortise-tenon joints.

2 Joint Design

The example joint used to validate the concept of curved non-sequential mortise-tenon joints of this research is modified from the top node joint of the full-scale non-sequential timber structure in [10]. In that practical scenario, the node connects a vertical member under tension with two horizontal members under compression. The present work modifies this node by replacing the straight mortise-tenons with curved ones, thereby improving structural robustness while preserving the reversibility of the original concept.

2.1 Geometry

As shown in Figure 1 c, the tenons on the left beam and the column have the shape of a circular arc, where the inner and outer arc share the same center. This ensures the insertion can be done when the left and right beams are rotating around their centers of the arcs.

The shape of the mortise and tenon between the left beam and the right beam is determined by the relative movement trajectory of the right beam with respect to the left beam, as they rotate simultaneously around their respective centers. This trajectory can be described in the polar coordinate system of the left beam by Equation (1),

$$r(\psi) = a + b \cdot \cos\psi, \quad (1)$$

which is the standard form of the Limaçon of Pascal [15]. With parameters $a = 8$ and $b = 8\sqrt{2}$, the condition $b > a$ is satisfied. Consequently, the trajectory forms a limaçon with an inner loop, which results in the hook-like shape of the peg between the left beam and the right beam.

The final tenon shape with tapering is optimized numerically by simulating two rigid bodies rotating around two centers separately and calculating the gaps at each side of the tenon at each time step.

2.2 Advantages

2.2.1 Stress Distribution under Bending

The curved mortise-tenon offers a larger contact area and enables better stress distribution compared to straight tenons in bending. Figure 1 d shows that when a bending load is applied, the forces are transferred through bearing contact across the curved surface [16], rather than concentrating at a single pin or edge of a straight tenon [17][18][19][20]. The lever arm OA' is longer than OA due to the angle of contact pressure, resulting in smaller stress at B' than at B.

To quantitatively support the claimed improvement in stress transfer under bending, an additional finite element analysis (FEA) was carried out in Ansys [21] for the proposed curved mortise-tenon joint and for a geometry-matched (equal mortise depth) straight mortise-tenon reference under the same bending moment (Figure 1 e). The two joints were evaluated under identical loading and boundary conditions, contact assumptions and material parameters so that the effect of the joint geometry could be isolated. The maximum von Mises stress reaches about 1.156 MPa in the straight tenon, compared with the approx. 0.771 MPa in the curved tenon, which corresponds to a reduction of approximately 33% in peak stress for the proposed curved joint. These results support the claim that the curved geometry improves stress distribution under bending. However, the present FEA comparison is intended as a preliminary numerical indicator of structural benefit and comprehensive mechanical bending tests remain part of future work.

2.2.2 Increased Contact Area

By curving the tenon (and corresponding mortise) along an arc, a longer continuous contact surface can be achieved even within a compact joint region, which can provide more friction force under loading.

2.2.3 Pull-Out Resistance

Conventional mortise-tenon joints primarily transfer load through bearing contact between tenon cheeks and mortise walls, which provides bearing capacity for shear actions perpendicular to the tenon axis and for rotational restraint depending on detailing [22]. In contrast, resistance against pull-out along the tenon direction mainly comes from tight-fit friction and is not treated comprehensively in common design standards such as Eurocode 5 [23].

Non-sequential mortise-tenon joints partially reduce the pull-out risk by combining multiple tenons oriented in different directions, such that no single straight translation can release the connection [9]. Nevertheless, if the locking relies on a small number of straight sliding directions, there remains a residual failure mode in which parts can gradually migrate along their insertion directions under repeated vibrations (e.g. wind, operational loads, or seismic excitation), especially if friction decreases due to wear or moisture changes.

The proposed curved non-sequential mortise-tenon joint addresses this weakness. Disassembly is only possible if the members follow a specific curved extraction trajectory with coordinated relative motion, making unintended separation highly unlikely under realistic vibration, as random excitations cannot reproduce the necessary path and coordination.

2.2.4 Robotic Assembly

Straight mortise-tenon joints rely on tight-fit to provide friction against pull-out loads, which imposes high demands on robotic assembly, since millimeter-level positioning errors can lead to jamming, excessive insertion forces, or surface damage. Contrarily, the proposed joint with curved tenons maintains stability by form closure (geometric lock) rather than high friction. In fact, a properly designed non-sequential joint needs only minimal friction for stability. Therefore, the mortise and tenon need not be perfectly tight-fit and larger tolerance can be designed to ease the robotic assembly.

2.3 Disadvantages and Limitations

2.3.1 Manufacturing Complexity

The joint components with curved mortise-tenon profile are fabricated from timber with CNC milling, which does introduce some complexity in manufacturing.

2.3.2 Assembly Path Requires Space

The robot must follow a curved rather than straight path, which may require more space around the joint.

2.3.3 Friction Dependence

The assembly relies on friction characteristics being within a reasonable range. If the wood surface or finishes result in extremely high friction, the insertion might require more force than the robots can safely apply, or the joint might seize mid-way.

2.3.4 Complexity of Robotic Control

Orchestrating two robots simultaneously is inherently more complex than single-arm operations. The curved tenon shape increases the complexity of the planned trajectories of the robots and the difficulty of adjustment when jamming happens. Besides, as the control is based on trained RL policies, any changes in joint design or robot model would necessitate re-training. This could be a barrier for adapting the method to new projects without significant computational resources.

2.3.5 Grain Anisotropy

Wood exhibits significantly greater strength and stiffness parallel to the grain than perpendicular to it, and both tensile and shear resistance can be much lower when forces act across grain directions [24]. For the proposed joint, this implies that using homogeneous timber may cause local strength problems for the curved tenons due to grain anisotropy. Therefore, Cross Laminated Timber (CLT) [25] or similar engineered timber with cross-grain layers need to be used to ensure reliable load transfer and joint bearing capacity.

3 Robotic Assembly Strategy

To assemble the curved joint, two Franka Research 3 robotic arms work in synchronization. Each robot grasps one timber part. The third part is fixed as the existing structure. The use of two robots is motivated by the need for controlled motion of both parts: as the tenon begins to engage, both pieces must move simultaneously to negotiate the curved path. This is a coordinated, dynamic insertion where one robot's motion relative to the other is constrained by the joint geometry. In effect, the robots perform a "handshake" maneuver, each contributing to the relative motion required for mating the joint.

3.1 Initial Alignment

Before insertion, a computer vision system detects the AprilTag on the fixed part and provides an estimate of the part's pose (position and orientation) in the robot coordinate frame. This yields an initial alignment with an accuracy of about ±1 mm in position and ±0.5° in orientation. No separate fine calibration step or jigs are used. The robots proceed directly to the insertion maneuver from this pose. The tolerance of the joint design with chamfered tenons, combined with the adaptive control policy using RL and impedance control, obviates the need for laborious pre-alignment or adjustment phases.

3.2 Synchronized Dual-Arm Motion

Once in position, the robots execute the insertion motion in a tightly coordinated fashion. In practice, the coordinated motion is achieved by having both robots follow a time-synchronized trajectory plan generated by the learned policy. At each time step, the policy outputs target motions for both arms simultaneously. The key challenge is maintaining the correct relative pose of the two parts throughout the motion: even a small deviation can cause one side of the tenon to bind against the mortise. This multi-point contact peg-in-hole problem demands continuous adjustment by both robots.

3.3 Force Accommodation

Purely rigid trajectory tracking during insertion is brittle under residual pose errors, unmodeled contact conditions, and friction variability, and can lead to excessive interaction forces or jamming. Therefore, a Cartesian impedance controller is applied to regulate the end-effector's apparent stiffness and damping so that small contact-induced deviations are compliantly absorbed while keeping forces bounded and avoiding surface damage. This yields a form of passive compliance that helps prevent jamming. If the tenon presses hard on one side, the fixture deflects a few millimeters to relieve pressure until the policy can correct the course. Both robots adjust their trajectories based on current poses and sensed forces, maintaining a balanced insertion where contact forces remain below a safe threshold.

After each tenon fully reaches the end of the curved slot, the joint is locked in place. The robots then release the components. The connection can later be disassembled by reversing the motion: the robots re-grip the parts and withdraw them along the same curved path. This reversible assembly process is repeated multiple times in the experiments to validate the joint's reusability.

4 Reinforcement Learning Policy

4.1 Algorithm

The Proximal Policy Optimization (PPO) [26] algorithm is utilized as the learning algorithm for the robot control, owing to its stability and good performance on continuous control tasks. The applied PPO algorithm is based on the Brax implementation [27].

The reward function consists of a position-based insertion progress term $r_{i,\mathrm{prog}}$ and an angular alignment term $r_{i,\mathrm{align}}$ for each mortise-tenon pair $i \in \{1,2,3\}$, together with a terminal success reward, a terminal penalty for excessive joint torque, a penalty on joint-space deviation from initial pose to improve efficiency, and a synchronization penalty to reduce dual-arm mismatch during insertion. The total reward is defined as

$$r = \sum_{i=1}^{3}\left(w_{i,\text{prog}} \cdot r_{i,\text{prog}} + w_{i,\text{align}} \cdot r_{i,\text{align}}\right) + w_{\text{succ}} \cdot I_{\text{succ}} - w_{\text{torq}} \cdot I_{\text{torq}} - w_{\text{effi}} \cdot r_{\text{effi}} - w_{\text{sync}} \cdot r_{\text{sync}}, \quad (2)$$

where w is weight factor and the insertion and alignment terms are given by

$$s_{i,\text{prog}} = \left\|\boldsymbol{p}_{i,\text{mortise}} - \boldsymbol{p}_{i,\text{tenon}}\right\|, \quad (3)$$

$$s_{i,\text{align}} = \left|\theta_{i,\text{mortise}} - \theta_{i,\text{tenon}}\right|, \quad (4)$$

$$r_{i,\text{prog}} = 1 - \tanh(w_p \cdot s_{i,\text{prog}}), \quad (5)$$

$$r_{i,\text{align}} = 1 - \tanh\left(w_\theta \cdot s_{i,\text{align}}\right), \quad (6)$$

where $\boldsymbol{p}$ is position and θ is orientation. To discourage unnecessary motion, the joint-space deviation cost is defined as

$$r_{\text{effi}} = \tanh(w_{\Delta \boldsymbol{q}} \cdot \textstyle\sum_{a=1}^{2}\left\|\boldsymbol{q}_{a,\text{curr}} - \boldsymbol{q}_{a,\text{orig}}\right\|), \quad (7)$$

where $\boldsymbol{q}_{a,\text{curr},}$ is the current joint angles of robot arm a and $\boldsymbol{q}_{a,\text{orig}}$ is the original angles. To penalize mismatch between the two tenons that are symmetrical (i = 1 and 2), the synchronization cost is defined as

$$r_{\text{sync}} = \tanh(w_{\Delta\text{prog}} \cdot \left|s_{1,\text{prog}} - s_{2,\text{prog}}\right|). \quad (8)$$

In addition, $I_{\text{succ}} \in \{0,1\}$ is the success indicator, and $I_{\text{torq}} \in \{0,1\}$ is activated and the episode is terminated when any joint torque exceeds the predefined safety threshold.

The observation space consists of the joint angles and velocities of the two robot arms, the current Cartesian pose of the two grippers and the measured joint torque of the two arms due to restraint, for which a low-pass filtering is conducted and both the filtered and unfiltered torques are used for observation. The actions are the Cartesian translational and rotational movements of the two grippers for each timestep.

4.2 Training in MuJoCo Simulations

A physics simulation of the two robots and the timber joint is developed in MuJoCo [28], which is a high-fidelity simulator that can incorporate robot dynamics and contact physics for wood-wood interaction (Figure 2). MuJoCo Playground [29] is used as the training stack to allow parallelization of environments on GPU. Each training has 200 million iteration steps and 8192 parallel environments and takes about 5 hours for a single Nvidia A100 GPU node. The simulation is slower than typical MuJoCo simulations as the contact dynamics are intentionally modeled as very stiff, requiring a small timestep (0.0005 s) and high solver iteration count (250) to ensure convergence of the contact forces. As a result, the computational cost is highly sensitive to the contact stiffness, timestep, solver iterations, and domain-randomization settings. When adapting the method to similar but different geometries, the retraining effort is expected to remain moderate, since the proposed joints are constructed from simple parametric curves such as circular arcs, which limits the exploration complexity of PPO. Moreover, multiple joints within the same project may share the same underlying geometric principle, reducing the need for retraining and making warm-start fine-tuning from a baseline policy a practical alternative to training from scratch.

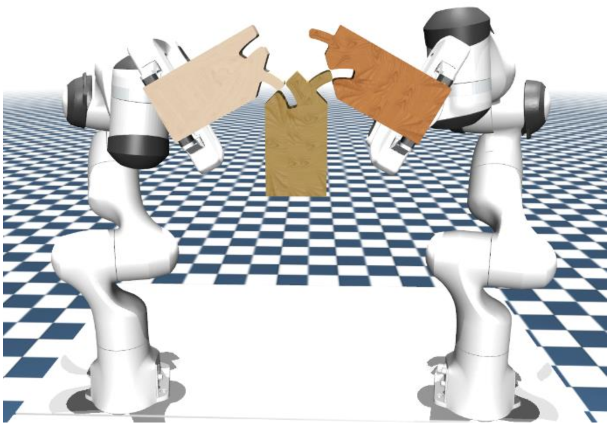

Figure 2. MuJoCo simulation.

4.3 Domain Randomization

A critical component of training is domain randomization, which is applied extensively to bridge the reality gap and ensure robustness. Table 1 summarizes the key parameters randomized during simulation episodes. By exposing the learning agent to these variations, it could be ensured that the final policy was not tuned to a single ideal scenario but rather could generalize to the messy real-world conditions.

Table 1. Domain Randomization Ranges in Training

Parameters	Variation Range
Mass and inertia	±20%
Surface friction	0.1 – 0.7
Initial pose offset	±1.0 mm, ±1°
Base compliance	From very stiff to rigid

The mass of the two timber parts handled by the robots is varied within ±20% of their nominal values. The coefficient of friction between the contact surfaces is randomized from 0.1 to 0.7, because wood friction can differ due to surface finish or humidity, etc. Small random offsets up to ±1 mm and ±1° in random directions are added to the initial alignment of the parts, simulating errors in AprilTag localization or placement.

To model that real existing building components may not be fully rigid during assembly both in lab tests and on site, the stiffness of the simulated base holding the timber column is randomized from very stiff to fully rigid. In the training in MuJoCo, the base stiffness is varied from fully rigid to a specific stiffness, which is determined as the stiffness that when the robot is applying a horizontal force at its maximum payload, the fixed part is showing 0.5 mm deformation. The policy has to succeed across this spectrum, learning not to rely on the base being perfectly immovable.

5 Experiments

5.1 Setup

The system was validated in physical assembly experiments with the curved joint using two 7-degree-of-freedom Franka Research 3 robotic arms (see Figure 3 and [14]). Each arm has a maximum payload of 3 kg and was equipped with an eye-in-hand camera of the type RealSense D405 for the localization of the fixed timber components. This setup is not intended to directly represent full-scale structural deployment. Instead, it serves as an experimentally accessible platform to validate the curved non-sequential joint and the corresponding learning-based assembly strategy under controlled laboratory conditions.

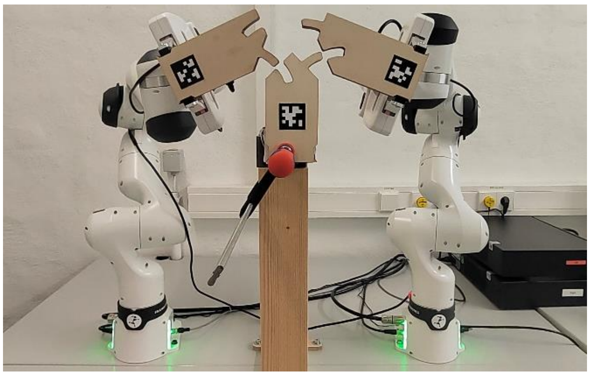

Figure 3. Hardware setup of the experiments.

Three sets of samples with different materials were prepared for real tests: timber, waxed timber and 3D-printed PLA. The waxed timber was smoother than timber and the 3D-printed parts had the smoothest surface. The samples were manufactured from laminated plywood boards consisting of multiple thin veneers bonded together with alternating grain directions, which reduces the prominence of grain-direction anisotropy at the scale of the assembly experiments.

Disassembly was tested by executing the recorded movements during assembly in reverse. A trial was considered successful when both the assembly and disassembly were completed within 40 s and without excessive contact forces. This threshold was introduced as an experimental evaluation criterion based on observations to separate successful executions from cases with prolonged self-correction or near-stagnation. It should not be interpreted as a target construction cycle time for practical on-site deployment.

5.2 Results

The learned RL policy proved capable of consistently assembling and disassembling the joint without human intervention [14]. As summarized in Table 2, a success rate of more than 90% was achieved. The typical insertion took about 15 s, whereas the disassembly took about 10 s. As expected, the tighter fit (0.2 mm) on raw timber was slightly less reliable than a looser 0.3 mm fit and required more assembly time due to more recovery motions. However, when the timber was waxed (lower friction), the 0.2 mm clearance performed almost as efficiently and robustly as a looser fit. This trend is further supported by the 3D-printed parts: despite a gap of only 0.1 mm, their smoothness and geometric precision yielded high success and acceptable assembly time. The high standard deviation (SD) in assembly time of Groups 2–4 is due to the many recovery attempts due to the tight-fit gap. Overall, these observations suggest that the RL policy can accommodate small clearances, but extremely tight fits may still risk occasional hang-ups unless friction is mitigated.

Table 2. Results of real tests

Group	1	2	3	4
Material	Timber	Timber	Timber (waxed)	3D-Print
Tolerance [mm]	0.3	0.2	0.2	0.1
Successful Trials [-]	20/20	18/20	19/20	19/20
Min. Time* [s]	12.3	12.6	12.5	13.1
Max. Time* [s]	16.5	33.2	39.7	38.5
Mean Time* [s]	14.4	16.8	15.5	16.1
SD Time* [s]	1.1	5.5	6.4	5.7

* Computed over successful trials.

Figure 4 illustrates the rotational angles of the timber parts relative to the target orientation of six typical trials in the real tests, which represents the progression from initial pose (0°) to full insertion (28°). The trials begin in slightly misaligned states due to the AprilTag pose estimation error. A typical successful assembly is shown by Trial 3, which took about 12.5 s. Trial 4 shows a situation in which the policy encountered difficulty but succeeded in continuing the assembly after multiple self-correction attempts. Trial 1 and Trial 6 show the situation that one arm advanced deeper than the other and the controller performed a brief back-off with the leading arm to re-establish symmetric insertion depth. It then resumed forward motion with both arms synchronized and proceeded smoothly to full seating, although still categorized as unsuccessful due to exceeded assembly time. Trial 2 and Trial 5 show a representative failure case, in which the policy tried to withdraw the tenons after entering a contact state from which it did not recover and reached torque limit. The tests show that the failure cases arise from out-of-distribution (OOD) contact states. In particular, small deviations in the actual pose, surface roughness, and geometric imperfections lead to joint torque and robot pose combinations that were insufficiently represented during training. In such states, the learned policy may either continue insertion, which increases resistance and triggers the joint-torque safety limit, or prematurely withdraw from a still-recoverable insertion state and abandon the assembly attempt.

In all successful trials, the joint could be disassembled without difficulty, confirming its reusability. Importantly, after multiple times of assembly and disassembly, the timber surfaces showed nearly no wear. This suggests that the learned gentle insertion strategy, combined with the chamfered edges and controlled contact forces, avoids significant damage to the wood.

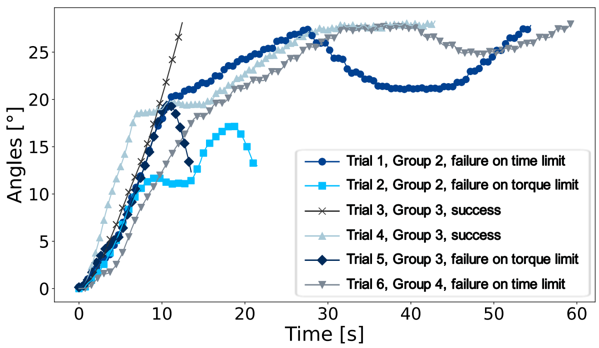

Figure 4. Rotational angles of timber parts in real tests.

6 Conclusion and Outlook

A novel curved mortise-tenon timber joint that enables non-sequential robotic assembly was introduced, along with a dual-robot RL-based assembly strategy. The curved and non-sequential joint design provides reusability and kinematic self-locking, and improves stress distribution under loading and is therefore ideal for robotic assembly and disassembly of timber structures. By training a PPO policy with extensive domain randomization, the robots successfully performed the complex multi-contact insertion without predefined alignment or force-control heuristics. The achieved success rate of more than 90% validates both the joint concept and the control approach.

Future work will explore improved joint geometries that simplify machining or further increase tolerance to wood expansion. In addition, mechanical tests will be conducted to validate the mechanical performance of the proposed curved joints. Integrating real-time vision or tactile feedback into the policy (e.g. through online learning or adaptation) could make the system even more robust to changes such as humidity or wear. Additionally, scaling up to full-scale timber assembly (e.g. with spider cranes as in [5]) and multi-joint assemblies (where a robot might assemble several of these connections on one component) is an important next step.

Acknowledgement

Supported by the Deutsche Forschungsgemeinschaft (DFG, German Research Foundation) under Germany's Excellence Strategy – EXC 2120/1 – 390831618.

The authors gratefully acknowledge the computing time provided on the high-performance computer HoreKa by the National High-Performance Computing Center at KIT (NHR@KIT). This center is jointly supported by the Federal Ministry of Education and Research and the Ministry of Science, Research and the Arts of Baden-Württemberg, as part of the National High-Performance Computing (NHR) joint funding program (https://www.nhr-verein.de/en/our-partners). HoreKa is partly funded by DFG.

References

[1] FIEC – European Construction Industry Federation. Position Paper: Shortage of Labour in the Construction Industry: 2025 edition. On-line: https://www.fiec.eu/application/files/1517/6331/6876/2025-11_FIEC_Position_Paper_labour_shortages.pdf, Accessed: 12/10/2025.

[2] L. Tupenaite, L. Kanapeckiene, J. Naimaviciene, A. Kaklauskas, and T. Gecys. Timber Construction as a Solution to Climate Change: A Systematic Literature Review. *Buildings*, 13(4):976, 2023.

[3] O. Bucklin, R. Di Bari, F. Amtsberg, and A. Menges. Environmental Impact of a Mono-Material Timber Building Envelope with Enhanced Energy Performance. *Sustainability*, 15(1):556, 2023.

[4] C. Brosque and M. Fischer. Safety, quality, schedule, and cost impacts of ten construction robots. *Construction Robotics*, 6(2):163–186, 2022.

[5] A. P. R. Lauer et al. Automated on-site assembly of timber buildings on the example of a biomimetic shell. *Automation in Construction*, 156:105118, 2023.

[6] A. P. R. Lauer, T. Schürmann, A. Gienger, and O. Sawodny. Force-Controlled On-Site Assembly Using Pose-Dependent Stiffness of Large-Scale Manipulators. In *2023 IEEE 19th International Conference on Automation Science and Engineering (CASE)*, Auckland, New Zealand, 2023, pages 1–6.

[7] L. Wu and A. P. R. Lauer. A lashing-mortise-tenon timber joint for automatic on-site assembly. In *Proceedings of the 14th Creative Construction Conference (CCC 2025)*, Zadar, Croatia, M. Hajdu, M. Skibniewski, and Z. Turk, Eds., 2025, pages 266–272.

[8] S. G. Hansen, A. Kunic, and R. Naboni. A reversible connection for robotic assembly of timber structures. *Engineering Structures*, 245:112795, 2021.

[9] J. Glath, R. Mesnil, M. Mimram, and O. Baverel. Non-sequential assembly of mortise and tenon joints. *Automation in Construction*, 154:104986, 2023.

[10] A. Rossi *et al.* Robotic Non-sequential Interlocking Assemblies. In *Design Modelling Symposium Berlin*, 1st ed., pages 434–444, 2024.

[11] T. Inoue, G. de Magistris, A. Munawar, T. Yokoya, and R. Tachibana. Deep reinforcement learning for high precision assembly tasks. In *2017 IEEE/RSJ International Conference on Intelligent Robots and Systems (IROS)*, 2017.

[12] A. A. Apolinarska *et al.* Robotic assembly of timber joints using reinforcement learning. *Automation in Construction*, 125:103569, 2021.

[13] N. Rogeau, V. Tiberghien, P. Latteur, and Y. Weinand. Robotic Insertion of Timber Joints using Visual Detection of Fiducial Markers. In *Proceedings of the 37th International Symposium on Automation and Robotics in Construction (ISARC)*, Kitakyushu, Japan, H. Osumi, Ed., 2020, pages 491–498.

[14] A. P. R. Lauer. Automatic Assembly of a Non-sequential Curved Mortise-Tenon Timber Joint with Reinforcement Learning. On-line: https://youtu.be/2O-nF20d-t0, Accessed: 03/28/2026.

[15] J. D. Lawrence. A Catalog of Special Plane Curves. Dover Publications, New York, 1972.

[16] S. Malek, A. Goodarzi, R. Parra, and P. Khoshkbari. Finite element analysis of glulam beams with transverse and longitudinal notches. In *World Conference on Timber Engineering (WCTE 2023)*, Oslo, Norway, K. A. Malo, A. Q. Nyrud, and K. Nore, Eds., pages 2724–2730, 2023.

[17] S. Siby, A. Münzer, R. Zimmermann, S. Aicher, and P. Grönquist. Experimental characterization of moment rotation behavior of reinforced disassemblable mortise and tenon joints. In *World Conference on Timber Engineering 2025*, Brisbane, Australia, K. Crews, G. Nolan, and K. Rischmiller, Eds., pages 1856–1865, 2025.

[18] J. M. Branco and T. Descamps. Analysis and strengthening of carpentry joints. *Construction and Building Materials*, 97:34–47, 2015.

[19] J. F. Miller and R. J. Schmidt. Capacity of pegged mortise and tenon joinery. Research report. Department of Civil and Architectural Engineering, University of Wyoming, 2004.

[20] R. J. Schmidt and C. E. Daniels. Design considerations for mortise and tenon connections. Research report. Department of Civil and Architectural Engineering, University of Wyoming, 1999.

[21] ANSYS, Inc. *Ansys® Academic Research Mechanical* [Computer software], Release 2024 R2. Canonsburg, PA, USA: ANSYS, Inc., 2024.

[22] J. M. Branco, M. Verbist, and T. Descamps. Design of three Step Joint typologies: Review of European standardized approaches. *Engineering Structures*, 174:573–585, 2018.

[23] *EN 1995-1-1:2004 Eurocode 5: Design of timber structures – Part 1-1: General – Common rules and rules for buildings*, European Committee for Standardization, Brussels, 2004.

[24] T. Hirai. Anisotropy of Wood and Wood-based Materials and Rational Structural Design of Timber Constructions. In *The Proceedings of Design & Systems Conference*, 2005.15(0):19–22, 2005.

[25] V. de Araujo *et al.* Is Cross-Laminated Timber (CLT) a Wood Panel, a Building, or a Construction System? A Systematic Review on Its Functions, Characteristics, Performances, and Applications. *Forests*, 14(2):264, 2023.

[26] J. Schulman, F. Wolski, P. Dhariwal, A. Radford, and O. Klimov. Proximal Policy Optimization Algorithms. On-line: https://arxiv.org/pdf/1707.06347, Accessed: 12/10/2025.

[27] C. D. Freeman, E. Frey, A. Raichuk, S. Girgin, I. Mordatch, and O. Bachem. Brax - A Differentiable Physics Engine for Large Scale Rigid Body Simulation: version 0.13.0. On-line: http://github.com/google/brax, Accessed: 12/10/2025.

[28] E. Todorov, T. Erez, and Y. Tassa. MuJoCo: A physics engine for model-based control. In *2012 IEEE/RSJ International Conference on Intelligent Robots and Systems*, Vilamoura-Algarve, Portugal, pages 5026–5033, 2012.

[29] Google-deepmind. MuJoCo Playground: An open-source framework for GPU-accelerated robot learning and sim-to-real transfer: version 0.0.4. On-line: https://github.com/google-deepmind/mujoco_playground, Accessed: 12/10/2025.